

The Effect of Strain Path on the Microstructure and Mechanical Properties in Cu Processed by COT Method

Kinga Rodak

Silesian University of Technology Katowice,
Poland

1. Introduction

In recent years a lot of place in research has been devoted to the methods of grain refinement with the aid of large plastic deformations- *Severe Plastic Deformation*. The research of the methods of grain refinement is carried out in parallel to the intensive research of the structural changes occurring in the deformed materials. Some metallic materials which are deformed by means of *Severe Plastic Deformation* are characterized by ultrafine-grained and sometimes even nanograined size. Grain refinement fosters, above all, the increase in the strength of a material. Therefore, a production of nano- and ultrafine-grained structures has become one of the most important research issues which are currently the subject of interest in many research facilities. There are many techniques of SPD, for example: *Equal Channel Angular Pressing* (ECAP), *High Pressure Torsion* (HPT), *Cyclic Extrusion Compression* (CEC), *Hydroextrusion* (HE), the KOB methods, *Accumulative Roll Bonding* (ARB). The SPD techniques cannot be described as easy ways of obtaining the refined materials mainly because of the insufficient homogeneity of the structure, the low efficiency of the applied methods, and substantial losses of the material [Pakiela, 2009; Olejnik, 2005; Cao 2008]. That is why, the commonly know methods of SPD, excluding some exceptions [Bochniak, 2005], have not become implemented as production technologies, although a lot of time has passed since they were discovered. This is the reason why more and more works concentrate on using SPD techniques to produce a structure that is more homogenous and has higher degree of refinement [Shaarbaf, 2008; Raab, 2004]. There also appear some suggestions to modify SPD techniques [Lugo, 2008; Kulczyk, 2007]. Some intensive research is carried out aiming at preparing new SPD techniques which would have refined a grain to the level of ultrafine-grained or even nano-grained. One of such methods is the *Compression with Oscillatory Torsion* (COT). The method is regarded as an unconventional way of volume shaping and is developed by the Department Of Materials Technology in the Faculty of Materials Engineering and Metallurgy of the Silesian University of Technology. This method has become recognized mainly as a method that enables deformation of the materials to values of large plastic deformations [Pawlicki, 2007], therefore, it is possible to obtain a refined structure. The benefits from applying the COT method are visible mainly in the aspect of reduction of work hardening effects (lowering of the plastic deformation work) [Grosman, 2006] and formation of a particular type of a

spatial configuration of defects in deformed material [Rodak, 2007]. It is, therefore, worth-exploring because of the attractive perspectives of using this method to form ultrafine-grained structures by using a suitable combination of deformation parameters (change of deformation path). It was proven that grain refinement in the COT method happens when the deformation parameters are suitably chosen. Among the parameters there are: torsional frequency f , compression velocity v , absolute strain $\Delta\epsilon$, and torsion angle α . An interesting observation coming from the longstanding research on the changes of the structures that accompany the COT torsion, is the fact that the effective deformation ϵ_f cumulated in a material is not the most important parameter thanks to which obtaining the suitably refined grains is possible.

2. Compression with oscillatory torsion (COT) method and deformation path

Compression with oscillatory torsion is a new method of plastic deformation in which the material is deformed as an effect of a changing deformation path. Fig. 1 is a schematic presentation of the COT set up. The facility for compression with oscillatory torsion consists of upper and lower anvils made from high-strength tool steel. Torsional straining was achieved by rotating the lower anvil, and compression was simultaneously achieved by linear strain from the lower anvil.

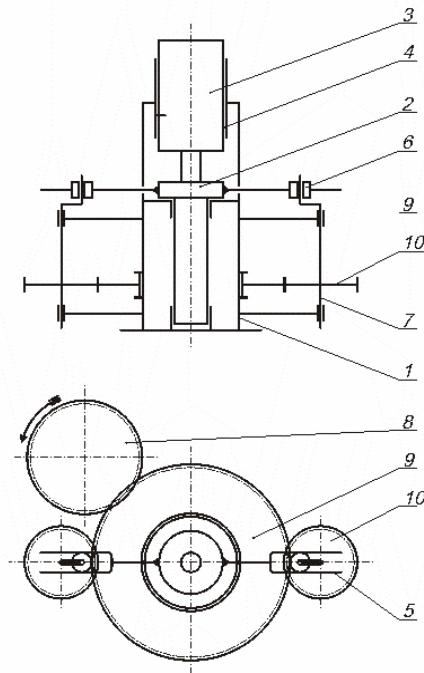


Fig. 1. Schematic illustration of COT process: 1. Frame, 2. Lower punch, 3. Upper punch, 4. Non-rotating slidable bearing, 5. Lower punch arm, 6. Roller, 7. Crankshaft, 8. Driving gear, 9. Ring gear, 10. Gear wheel

The appliance allows for the following parameters to change:

- the compression velocity v , (the velocity of the lower punch shift). The maximal value of compression velocity is 0,6 [mm/s]
- the torsional frequency f . The frequency of the lower punch oscillation is regulated by the inverter ranging from 0 Hz to 1,8 [Hz].
- the torsional angle amplitude α [°]. The set points of the kinematic magnitudes enable the change of the torsional angle ranging from 0° to 6°
- the absolute strain Δh [mm]
- the compression force F [kN]

The compressive force F and the deformation path are registered by computer. The process can be carried out only at room temperature.

The total cumulated value of deformation equals the sum of deformation dimensions obtained in consecutive cycles of torsion with simultaneous compression, for the following parameters: torsional velocity v , reversal torsional frequency f , amplitudes of the torsional angle α , the initial height of the test piece h_0 , the diameter of a test piece d_0 .

The total equivalent deformation ε_f is [Grosman, 2006]:

$$\varepsilon_f = \varepsilon_h + \varepsilon_t \tag{1}$$

where:

ε_h - the effective deformation from compression

ε_t - the effective deformation from torsion

This method regarded as an unconventional way of forming, has become recognized above all as an effective way to lower the force of plastic forming of a material. The force characteristics of the process depend on the component deformations induced by the torsion and compression. The value of the component deformations induced by the torsion is dependent on: torsional angle a and torsional frequency f . The component deformations induced by the compression are dependent on the compression velocity v . The proportions of the particular components describe the deformation path d_e [Grosman, 2006].

For the constant value of the torsional angle amplitude ($a = \text{const}$) the deformation path is proportional to the value of the torsional frequency to compression velocity ratio.

The force characteristics $F = f(\Delta h)$ indicates the raise of the torsional frequency f , accompanied by the constant values of the other process parameters: the absolute strain Δh , the compression velocity v and the torsional angle a , has an impact on the decrease of the axial (compression) force level (Fig.2). The course of curves shows that the double raise of the torsional frequency influences the lowering of the compression force more than 1,5 times and, additionally, reduces the work hardening. Higher torsional frequencies, in connection with the increased compression velocities, have no greater influence on the change of the average unit pressure.

In the method of compression with oscillatory torsion, a various combinations of the parameters can be used in order to obtain comparable values of the effective deformations.

The table 1. shows an example set of the deformation parameters needed to obtain similar values of the total effective deformation $\varepsilon_f \sim 5$ and ~ 14 . For the constant values of the $\Delta h = 3$ mm and the torsional angle $\alpha = 6^\circ$, the proportions between the compression velocity v and the torsional frequency f were changed. The effective deformation ε_f and the axial forces of compression are close to the test carried on with $f = 0,1$ Hz, $v = 0,015$ mm/s and $f = 0,8$ Hz, $v = 0,04$ mm/s. Likewise, for the test with $f = 0,2$ Hz, $v = 0,015$ mm/s and $f = 1,6$ Hz, $v = 0,04$ mm/s similar values of an effective deformation ε_f and the axial forces of compression are obtained. Yet, with such parameters higher effective deformations and lower axial forces of compression are achieved.

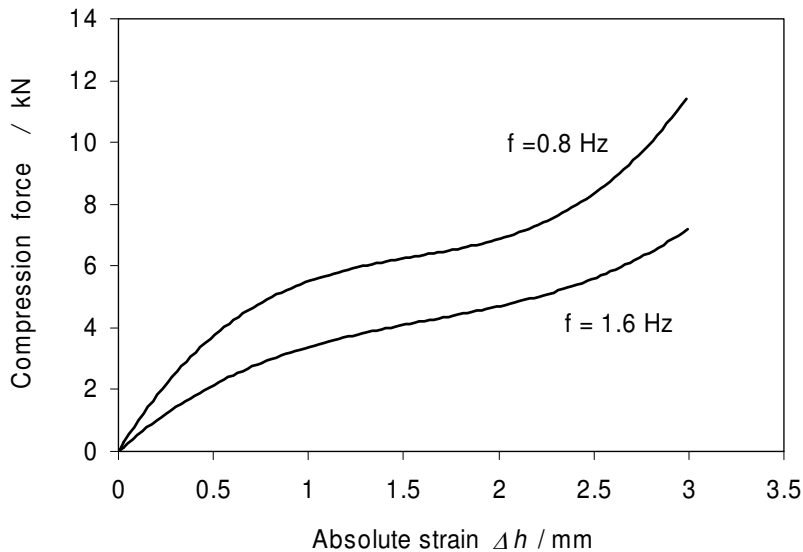


Fig. 2. Dependence of $F=f(\Delta h)$ for samples 3 and 4

Sample	1	2	3	4
	$\Delta h = 3$ mm	$\Delta h = 3$ mm	$\Delta h = 3$ mm	$\Delta h = 3$ mm
	$\alpha = 6^\circ$	$\alpha = 6^\circ$	$\alpha = 6^\circ$	$\alpha = 6^\circ$
Parameters	$f = 0.1$ Hz	$f = 0.2$ Hz	$f = 0.8$ Hz	$f = 1.6$ Hz
	$v = 0.015$ mm/s	$v = 0.015$ mm/s	$v = 0.04$ mm/s	$v = 0.04$ mm/s
Effective strain, ε_f	~ 5	~ 14	~ 5	~ 14

Table 1. Deformation parameters of Cu

The structural effects produced by the deformation with such parameters are interesting (Fig.3). Because of the possibility of using the COT method to refine the grain, more effective process is the one of deformation implemented by the use of higher parameters f and v , even for the comparable values of the effective deformations and the values of the axial forces of compression.

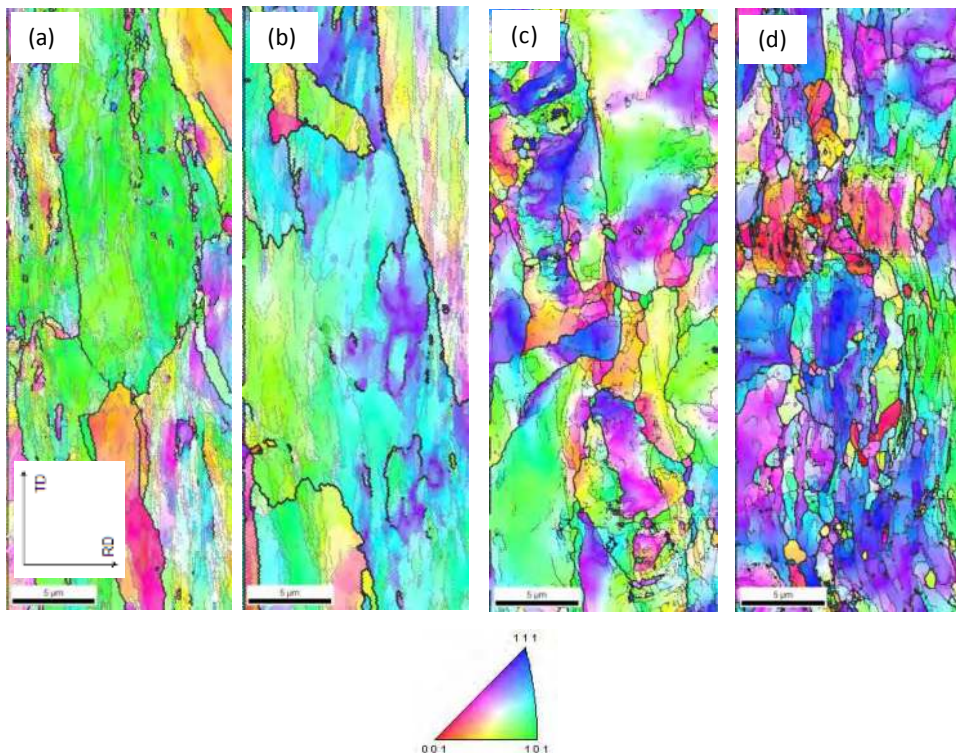


Fig. 3. EBSD maps of Cu after COT processing: a) sample 1, b) sample 2, c) sample 3, and d) sample 4

The deformation realized using high torsional frequencies evoked a decrease of the axial forces of compression in the material (Fig.2.) and the desired structural effect in a form of the grain refining (Fig.3). A similar correctness in a form of structural effects, was not observed in the case of deformable samples with small oscillating frequencies, in spite of the fact that also in this case a comparable decrease of the axial force level was registered. The conclusion might be that the effect of the decrease of the axis force and the increase of the effective deformation is not adequate with the structural effect in a form of grain refining.

In the COT method only the „special” conditions of the process (the proportions of the deformation parameters) can guarantee the effective grain refining. Therefore, the selection of the appropriate deformation parameters guarantee the effective grain refining.

3. Experimental details

The tests were conducted on the samples from copper in the M1E species (chemical composition is shown in the Table.2). This material is eagerly used to refine grains using the SPD techniques therefore, in case of new SPD techniques can constitute a good comparative material especially when it comes to the effectiveness of grain refining as well as to the mechanisms of grain refining process.

Chemical composition [%]						
Cu	Fe	Bi	Pb	Ni	Sn	As
99,8	0,02	0,002	0,008	0,019	0,03	0,001

Table 2. Chemical composition Cu used in experimental

The samples for the tests were taken from the bars having 12 mm in diameter and then, they were exposed to the heat treatment which involves the annealing in temperature of 500°C / 2 hours. After this treatment the average diameter of the grain equaled 50 μm . The heating treatment that was carried out, allowed for eliminating structural effects resulting from the previous technological treatments and for obtaining the homogenous grain structure in the whole volume of the material.

The test of compression with oscillatory torsion, required two types of samples. The first series of samples was prepared according to the scheme shown in the Fig. 4, where the ratio of height h (6 mm) to the diameter d (6 mm) equaled $(h/d) = 1$. Whereas, in the second set the height h was increased to 9 mm without the change of diameter and this equaled: $(h/d) = 1,5$.

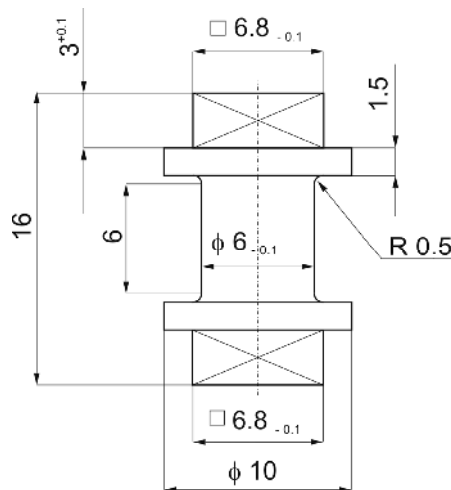


Fig. 4. Geometry and dimensions of samples used in the experiment

The deformation by means of the COT method was conducted using the following parameters:

- the range of the compression velocity; 4 variants of velocity were used: 0,015 mm/s; 0,04 mm/s; 0,1mm/s, 0,6 mm/s.
- the constant values of the torsional angle $\alpha=6^\circ$.
- the range of torsional frequency; 4 variants of this parameter were used: 0,2 Hz, 0,8 Hz, 1,6 Hz and 1,8 Hz.
- the absolute strain was $\Delta h = 3$ mm and $\Delta h = 7$ mm correspondingly for $(h/d) = 1$ and $(h/d) = 1,5$.
- the compression force F equaled 300 kN.

The compression with oscillatory torsion method is regarded as a method characterized by the heterogeneity of deformation. The most intense deformations proceed in places that are the nearest to the lateral surfaces of the material, which is results from the functioning of the torsional moment. The heterogeneity of the plastic deformation in the sample, causes the occurrence of a considerable differentiation of the structure in its sectional view. Because of the heterogeneity of the deformation, the microscope observations and strength testing were carried out in spheres located in a distance of about 0,8 of the sample's ray (Fig.5).

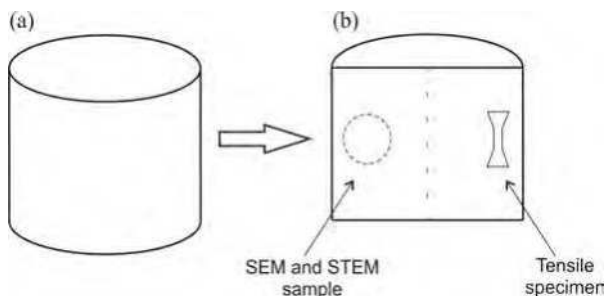


Fig. 5. Simple schematic of a specimen without the collar and handle: (a) sample after processing and (b) procedures for different types of testing: SEM and STEM observations and tensile testing using miniature specimens. The structure and mechanical properties studies were conducted on samples extracted from a distance near 0,8 radius in the longitudinal plane section

The analysis of the dislocating structure was carried out using the Scanning Transmission Electron Microscopy (STEM) technique which was applied thanks to the microscope Hitachi HD 2100A equipped with the FEG gun, working at the accelerating voltage of 200 kV.

With the help of Transmission Electron Microscopy (TEM) Jeol 100B, the orientation of the grains were determined based on the received pictures of Kikuchi lines. For the calculations the KILIN programme was used that was developed on the University of Science and Technology in Cracow.

The detailed quantities research of the ultrafine-grained structures being formed was conducted using Scanning Electron Microscope (SEM) INSPECT F produced by FEI equipped with the gun with cold field emission and the detector of electron back scattering diffraction (EBSD). In order to release the structure of the material by using the SEM/EBSD method, firstly, the mechanical polishing was used and then, electrolytic.

On the basis of the SEM/EBSD method the average equivalent diameter of the subgrains d [μm] and the average equivalent diameter of the grains D [μm] were determined. The boundary between the grain and subgrain was determined on the basis of the misorientation angle measurement. The divisional boundary was an angle equaling 15° . In the measurements of the average diameter of grain/subgrain, the grains located in the periphery of the image were not considered.

Some measurements of misorientation angles between the neighboring subgrains/grains were also taken. Therefore, the fields that had the misorientation degree from 2° were analyzed.

The estimation of the dislocation density in the material that were strongly deformed by means of transmission electron microscopy is almost impossible when these dimensions exceed $5 \cdot 10^{14} \text{ m}^{-2}$, and the result have a doubtful statistic value because of the small area of the analysis. Those inconveniences can be avoided by using the X-ray structural analysis.

The analysis of the diffraction line profile is an effective tool needed to characterize the structures of the material which have defects in crystal lattice. The presence in the material of tiny crystallites and the lattice distortions, causes the widening of diffraction reflexes. Both the size of the crystallites and the lattice distortions can be determined in quantity by means of the Williamson-Hall method in which the basis of analysis in this method is the Full Width at Half Maximum (FWHM) of the reflex, and using the Warren-Averbach method based on analyzing the Fourier coefficient [Ungar, 2001].

The difficulties in analysis using these methods occur when the material consists of anisotropy of diffraction line broadening. In such a case, neither the half-value line nor the Fourier coefficient constitute the monotonic function of the diffraction vector $K = (2\sin\theta)/\lambda$, where θ - reflection angle, λ - X-ray wavelength. The replacement of K and K^2 in a classic procedure of Williamson-Hall and Warren-Averbach by the expression $K^{1/2}$ and K^2 allows for eliminating the influence of anisotropy of diffraction line broadening.

The measurements of the hardness were taken by the Vickers method using the hardness testing machine FM 700 produced by the Japanese company Future Tech coupled with the metallographical microscope. The test was carried out with the loading of HV0,2.

Applying the hardness measurement, when the small volumes of the material, usually with heterogeneous deformation are obtained in the laboratory tests, is fully justified. However, the method that describes the strength and plastic features is the static tensile test. In the case of a very small dimension of the sample obtained by the SPD methods, the tensile test can be conducted only on the micro samples. Using micro samples is connected with numerous technical inconveniences among which there are: the danger of implementing structural changes resulting from the preparation of the material for the tests, fastening of the samples and the axiality of the meter circuit. In the tests that are described here, the micro samples have the dimensions 1.20×0.3 and length 2.20. The cutting was made using the spark wire (the wire was 0,1mm thick) with an intense cooling in distilling water.

The tensile test was carried out by employing the universal testing machine with the screw drive equaling MTS QTest/10. This method is successfully introduced in measuring deformations of small samples by the Faculty of Materials Science and Engineering in the Warsaw University of Technology. The elongation of the samples is measured using the digital image correlation method. The method is based on comparing of the digital recording of the sample image before the deformation (the reference image) with the digital recording of the sample image after the deformation. The computer algorithm compares the images and describes the relocate of small areas within the tested surface. Thanks to this method the local and total deformations on the whole analyzed surface of the sample can be determined. The tensile test was conducted with the initial tension velocity equaling $2 \cdot 10^{-3}$ [1/sec].

4. The impact of the deformation parameters on the grain refining

4.1 The torsional frequency

Among the several changing parameters of the deformation used in the COT method, the torsional frequency is the factor which, when increased, has a beneficial influence on lowering the value of the compression force (Fig.2.). Moreover, the increase of this parameter causes that the material is deformed to large values of effective deformations. For example, when the torsional frequency is 0,2 Hz and 1,8 Hz with the constant parameters: $\Delta h=7$, $\alpha=6^\circ$, $v=0,015\text{mm/s}$; the effective deformation ε_f equals 15 and 130. The Cu microstructure with the increasing torsional frequency was presented in Fig.6a.

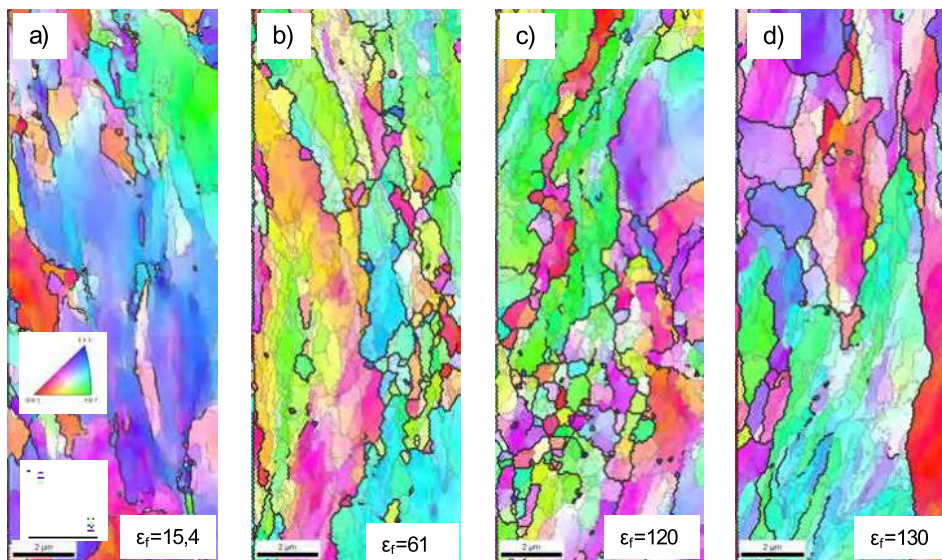


Fig. 6. EBSD maps of Cu after COT processing: a) $f=0,2$ Hz; b) $f=0,8$ Hz; c) $f=1,6$ Hz; d) 1,8 Hz at constant parameters: $\alpha =6^\circ$, $v=0,015$ mm/s i $\Delta h=7$ mm

The deformed copper with low torsional frequencies - 0,2 Hz is characterized mainly by the boundaries with a small misorientation angle. The boundaries like HABs are seen in the fragmentary outline. The Cu deformation with the increasing torsional frequency to 1,6 Hz, allows for the formation of the equiaxed structures having a great share of wide-angle boundaries (Fig.6b,c.). The maps obtained using the EBSD techniques show that the structures got during the deformation process where the torsional frequencies were - 0,8 Hz and 1,6 Hz, are characterized by the considerable grain refining, especially when it comes to the deformation when the torsional frequency was 1,6 Hz. It was observed that the numerous grains had the size no bigger than 1 μm . The neighboring grains are characterized by comparable but yet diversified crystallographic orientation. The great part of the analyzed surfaces are the banding structures isolated by high-angle boundaries and elongated in accordance with the direction of the compression. The example that are shown here prove that even if the values of effective deformations $\varepsilon_f=130$ are high, the microstructure Cu is characterized by heterogeneity.

The deformation of the material when the torsional frequency is $f = 1,8$ Hz produces an inconvenient phenomenon of developing large grains which often exceed $1 \mu\text{m}$.

This is proven by the results of the quantity tests of the grains and subgrains size (Fig.7), the area fraction of the grains with the misorientation above 15° and the size not exceeding $1 \mu\text{m}$, (Fig.8) and misorientation angle (Fig.9) that are fulfilling the ultrafine-grained material criteria.

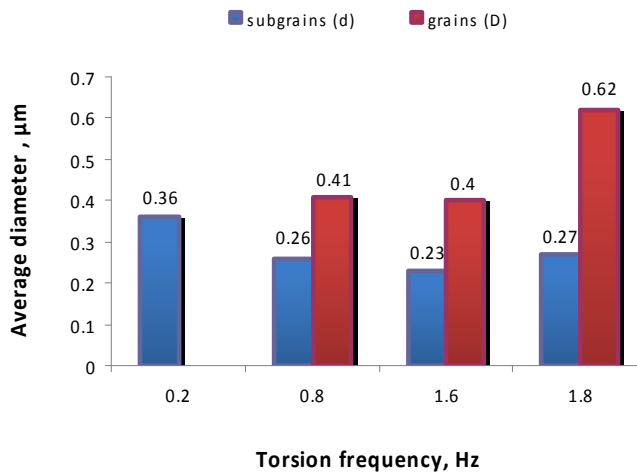


Fig. 7. The variation of the subgrain/grain size in dependence of changes in torsion frequency at constants: $\alpha = 6^\circ$, $v = 0,015$ mm/s, $\Delta h = 7$ mm

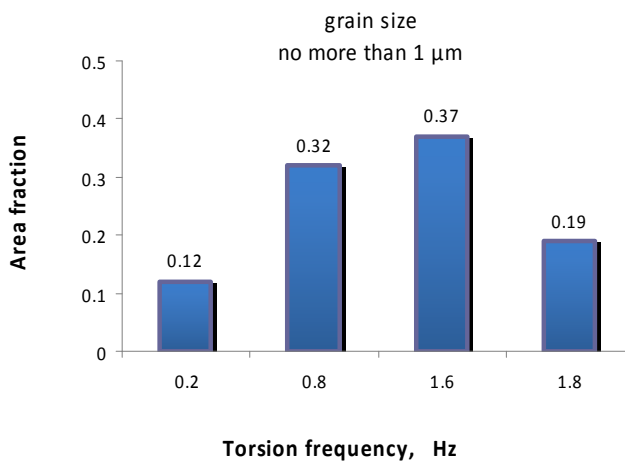


Fig. 8. The variation in the area fraction of ultrafine grain in dependence of changes in torsion frequency at constants: $\alpha = 6^\circ$, $v = 0,015$ mm/s, $\Delta h = 7$ mm

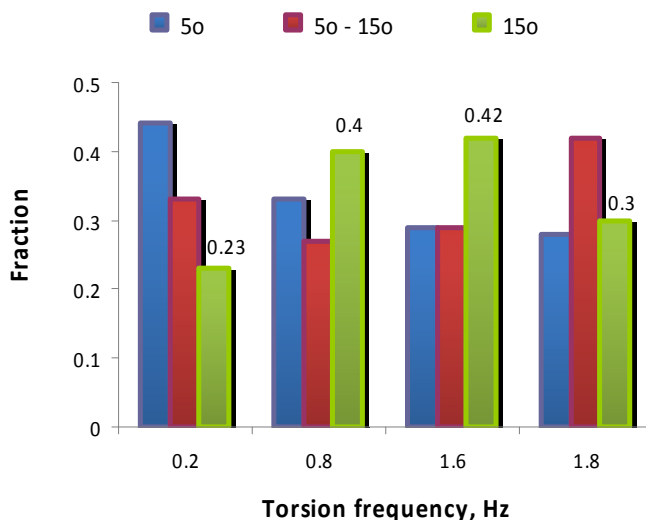


Fig. 9. The variation in the misorientation angle in dependence of changes in torsion frequency at constants: $\alpha = 6^\circ$, $v = 0,015 \text{ mm/s}$, $\Delta h = 7 \text{ mm}$

When the torsional frequency is 0,8 Hz and 1,6 Hz, the average diameters of the Cu grains have about 400 nm. A distinct increase of the average diameter of the grain is seen when the torsional frequency is increased from 1,6 Hz to 1,8 Hz. The grains have a size of about 600 nm. Roughly, it can be assumed that the subgrains are about 2 times smaller than grains. The area fraction of the grains to the magnitude of $1 \mu\text{m}$, also appears to be beneficial for the torsional frequencies 0,8 Hz and 1,6 Hz (especially for 1,6 Hz) (Fig.8.). The Cu grains which have the ultrametric size occupy about 40% of the analyzed surfaces. The application of the high torsional frequencies during the deformation process allows for obtaining about 40% of the high- angle boundaries fractions (Fig.9). It means that more than a half of the deformed structure is dominated by the subgrains.

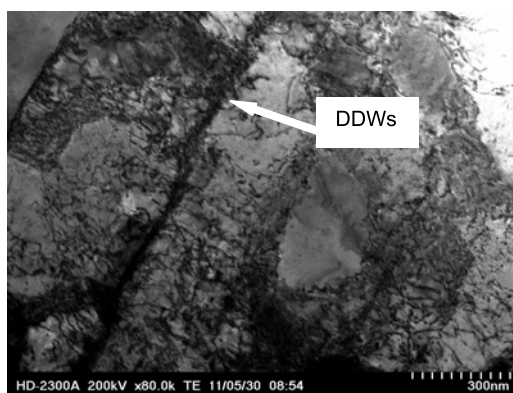


Fig. 10. Microstructure of Cu after COT deformation at: $f = 0,2 \text{ Hz}$, $\alpha = 6^\circ$, $v = 0,015 \text{ mm/s}$ and $\Delta h = 7 \text{ mm}$

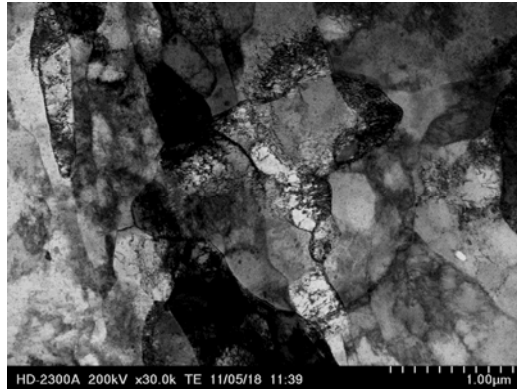


Fig. 11. Microstructure of Cu after COT deformation at: 11. $f=0,8$ Hz, $\alpha =6^\circ$, $v=0,015$ mm/s and $\Delta h=7$ mm

After the COT deformation with the torsional frequency $f=0,2$ Hz, the dislocation cell structure and the DDWs dislocation walls with a high density of dislocation are observed (Fig.10). The effects of arranging the dislocation structure are seen between the particular DDWs (Fig.10). In general, deformation carried out when the torsional frequencies are small makes the fraction of the narrow-angle boundaries (up to 5°) reaching almost 50% (Fig.9.) and the area fraction of the ultrafine-grains does not exceed 20% (Fig.8.).

It was observed that when the torsional frequency increased, the grain division into smaller volumes happened more often (Fig.11). The result of this is the generation of the greater amount of the LABs dislocation boundaries. A great amount of the tested areas of thin foils, shows that after the deformation with frequencies $f=0,8$ Hz and $f=1,6$ Hz in particular, the dislocation polygonal walls and the grains with the HAB boundaries are created in the structure (Fig.12). The vacancy clusters visible in Cu, are the effects of the dislocation annihilation (Fig.13). The results of measuring the dislocation density (Fig.14) are also the proof of the above mentioned.

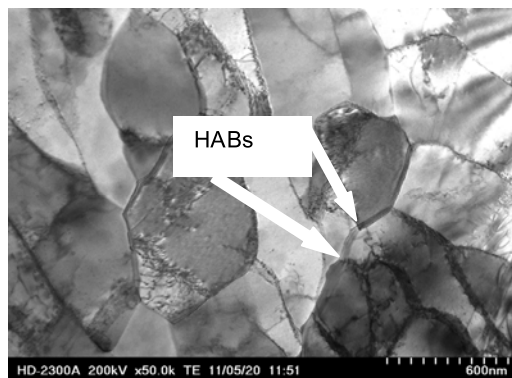


Fig. 12. Microstructure of Cu after COT deformation at: $f=1,6$ Hz, $\alpha =6^\circ$, $v=0,015$ mm/s and $\Delta h=7$ mm

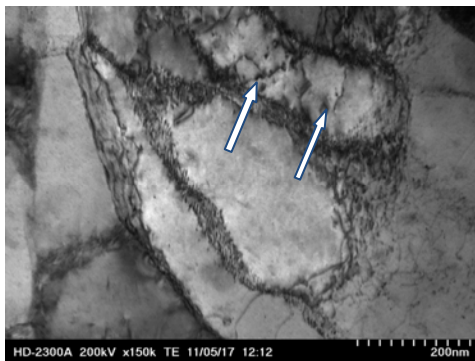


Fig. 13. Microstructure of Cu after COT deformation at: $f=1,6$ Hz, $\alpha =6^\circ$, $v=0,015$ mm/s and $\Delta h=7$ mm. The vacancy clusters are arrows marked



Fig. 14. Microstructure of Cu after COT deformation at: $f=1,8$ Hz, $\alpha =6^\circ$, $v=0,015$ mm/s and $\Delta h=7$ mm

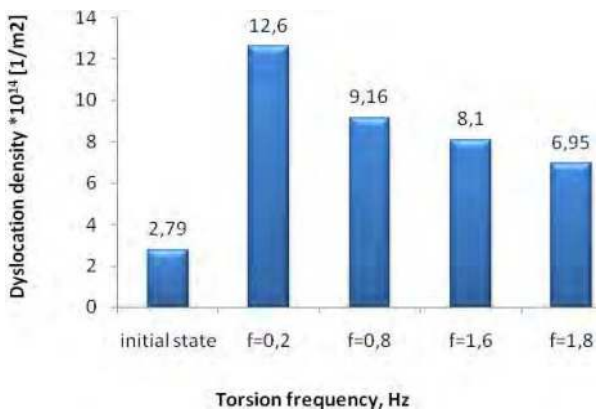


Fig. 15. The variation of the dislocation density in COTes samples with different value of torsion frequency and constant: $\alpha =6^\circ$, $v=0,015$ mm/s, $\Delta h=7$ mm

Together with the increase of the torsional frequency, the decrease of dislocation density is observed (Fig.15). When the frequency is 1,8 Hz the recovery begins to dominate the structure what has a negative influence on the material that is being refined (Fig.14). The transformation of dislocation tangles into polygonal boundaries and the dislocation annihilation, have no impact on raising the amount of the wide-angle boundaries fractions as well as on increasing the area fraction of the ultrafine-grains.

4.2 The compression velocity

In the COT process the compression velocity is the parameter which when increased, has an influence on highering the value of the compression force and on lowering the values of equivalent deformations. For example, the compression velocity 0,015 mm/s and 0,04 mm/s while the rest of the parameters is constant: 1,6 Hz, $\Delta h=7$, $\alpha=6^\circ$; the effective deformation ε_f is 120 and 45. Applying even higher compression velocities i.e. $v=0,1$ mm/s and $v=0,6$ mm/s causes a significant decrease of effective deformation to the corresponding values $\varepsilon_f=12$ and $\varepsilon_f=2$.

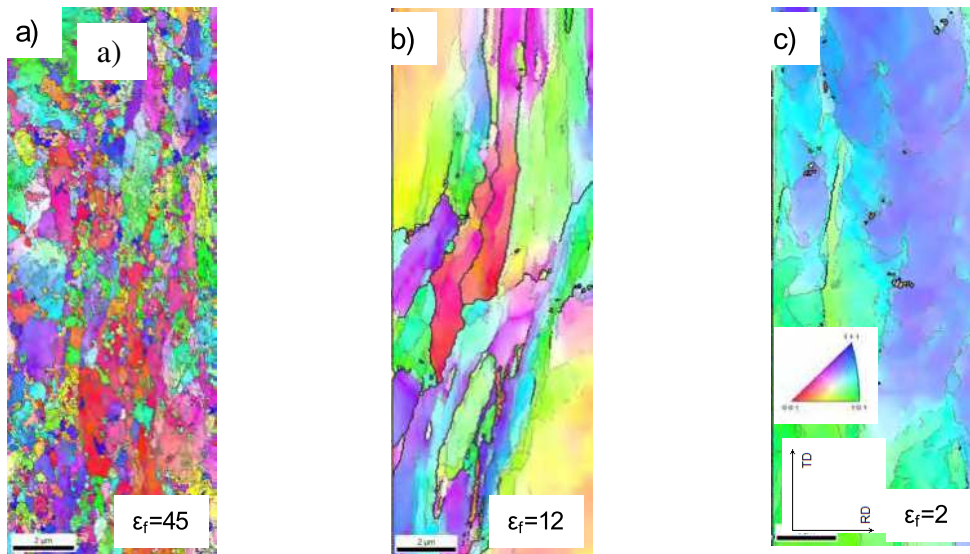


Fig. 16. EBSD maps of Cu after COT processing: a) $v=0,04$ mm/s; b) $v=0,1$ mm/s; c) $v=0,6$ mm/s; at constant parameters: $\alpha=6^\circ$, $v=0,015$ mm/s i $\Delta h=7$ mm

The deformation realized when the compression velocity is increasing from 0,015 mm/s to 0,04 mm/s while the rest of the parameters is constant: 1,6 Hz, $\Delta h=7$, $\alpha=6^\circ$; has an positive influence on the grain refining as well as on the increase of the homogeneity of the structure (compare Fig.6c and Fig.16a). The structures in the prevailing part of the areas are equiaxed, the grains bigger than 1 μm are not produced, the amount of high-angle boundaries is high. Whereas, the further increase of this parameter delays the reduction of the grain size and the creation of high-angle boundaries (Fig.16 b,c). During the deformation with the velocity of 0,1mm/s the effects of the structure deformation are clearly visible (Fig.16b), but when the

compression has the velocity of 0,6 mm/s only the fragments of the near-angle boundaries attest to the insignificant deformation of the material (Fig.16c). A significant reduction of the deformation realized by the increase of the compression velocity, does not lead to the grain refining.

When it comes to the Cu refined-grain, the juxtaposition of the structural changes for two velocities: 0,015 mm/s and 0,04 mm/s as well as of different torsional frequencies is quite interesting (Fig.17). That is why the further structural analysis involved comparing some selected ways of deformation.

Comparing the EBSD images obtained for Cu after the deformation with the compression velocity of $v = 0,015$ mm/s and $v = 0,04$ mm/s, the constant torsional frequency 1,6 Hz and the rest of the parameters also being constant (Fig.6c and Fig.16a), it is seen that the deformation happening at higher compression velocity is an effective way of grain-refining. It is also proven by the results of the quantity tests shown in the Figs.18-20. The average diameter of the Cu grain after the increase of the compression velocity, decreases from 400 nm to 300 nm (Fig.18). The average diameter of the subgrains also decreases from 230 nm to 180 nm (Fig.18). The area fraction of the grains up to 1 μm constitute 60% which is advantageous, when the torsional frequency is 1,6Hz and the compression velocity is $v = 0,04$ mm/s (Fig.19).

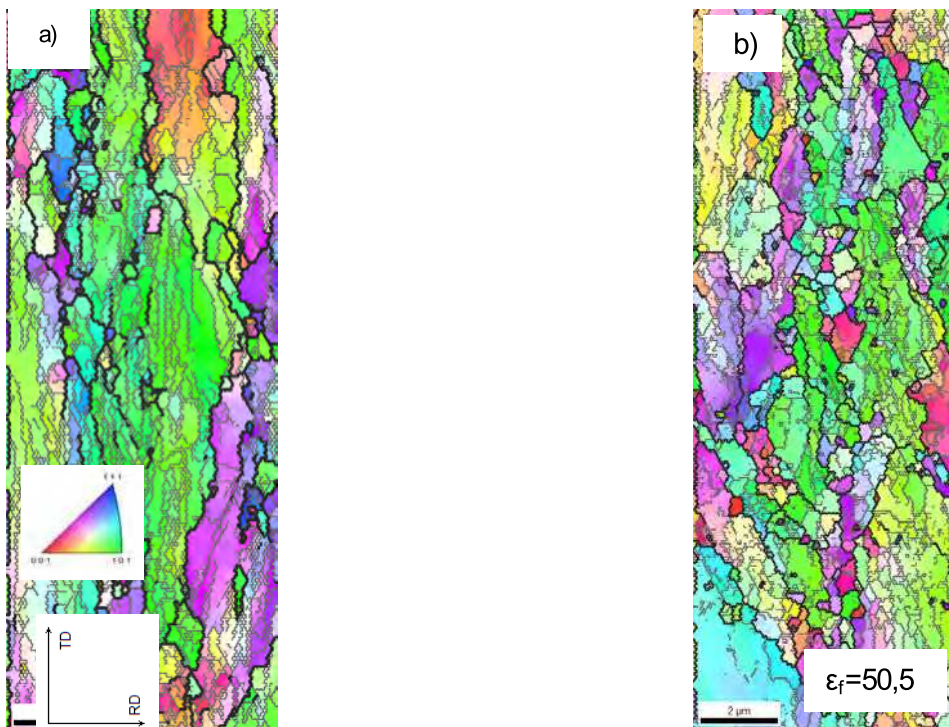


Fig. 17. EBSD maps of Cu after COT processing: a) $f=0,8\text{Hz}$; b) $f=1,8\text{Hz}$; at constant parameters $\alpha = 6^\circ$, $v=0,04$ mm/s and $\Delta h=7$ mm

When the compression velocity is higher, the high-angle boundaries are easily created and they constitute about 50% of the analyzed Cu areas (Fig.20).

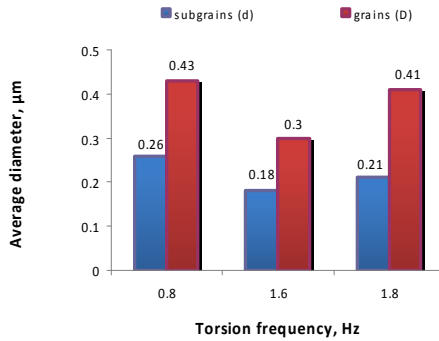


Fig. 18. The variation of the subgrain/grain size in dependence of changes in torsion frequency at constants $\alpha = 6^\circ$, $v = 0,04$ mm/s, $\Delta h = 7$ mm

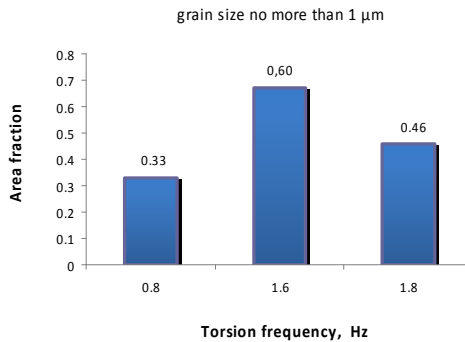


Fig. 19. The variation in the area fraction of ultrafine grain in dependence of changes in torsion frequency at constants: $\alpha = 6^\circ$, $v = 0,015$ mm/s, $\Delta h = 7$ mm

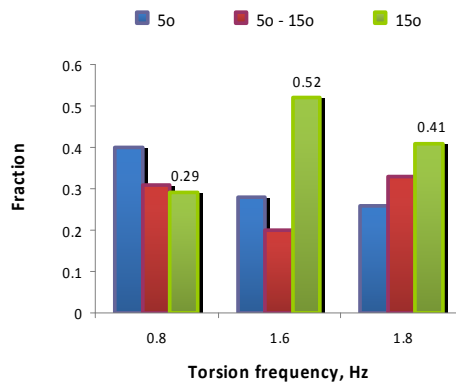


Fig. 20. The variation in the misorientation angle in dependence of changes in torsion frequency at constants: $\alpha = 6^\circ$, $v = 0,015$ mm/s, $\Delta h = 7$ mm

Comparing the structure of the deformed samples when the torsional frequency is lower - 0,8 Hz the compression velocities are as mentioned, it is visible that the Cu samples deformed with the higher compression velocity maintain greater fraction of the near-angle boundaries than the samples deformed with the lower compression velocity. The deformation realized when the compression velocity is $v = 0,015 \text{ mm/s}$ and $v = 0,04 \text{ mm/s}$ does not cause any significant changes when it comes to the size of the grains and subgrains (Fig.7 and Fig.18). The differences in the area fraction of the grains up to $1 \mu\text{m}$ were not observed (Fig.8 and Fig.19).

In the case of the deformation when the compression velocity was $0,04 \text{ mm/s}$ and the torsional frequency was $1,8 \text{ Hz}$, it was observed that Cu structure was significantly smaller than after the deformation with the compression velocity equaling $v = 0,015 \text{ mm/s}$ (Fig.6d and Fig.17b). The area fraction of the grains up to $1 \mu\text{m}$ are also greater (Fig. 19) as well as the high-angle boundaries fractions (Fig.20).

STEM micrographs (Fig.21) evidently demonstrate that deformation at higher value of v parameter leads to generating banded structure with low angle grain boundaries and high value of dislocation density (Fig.22).

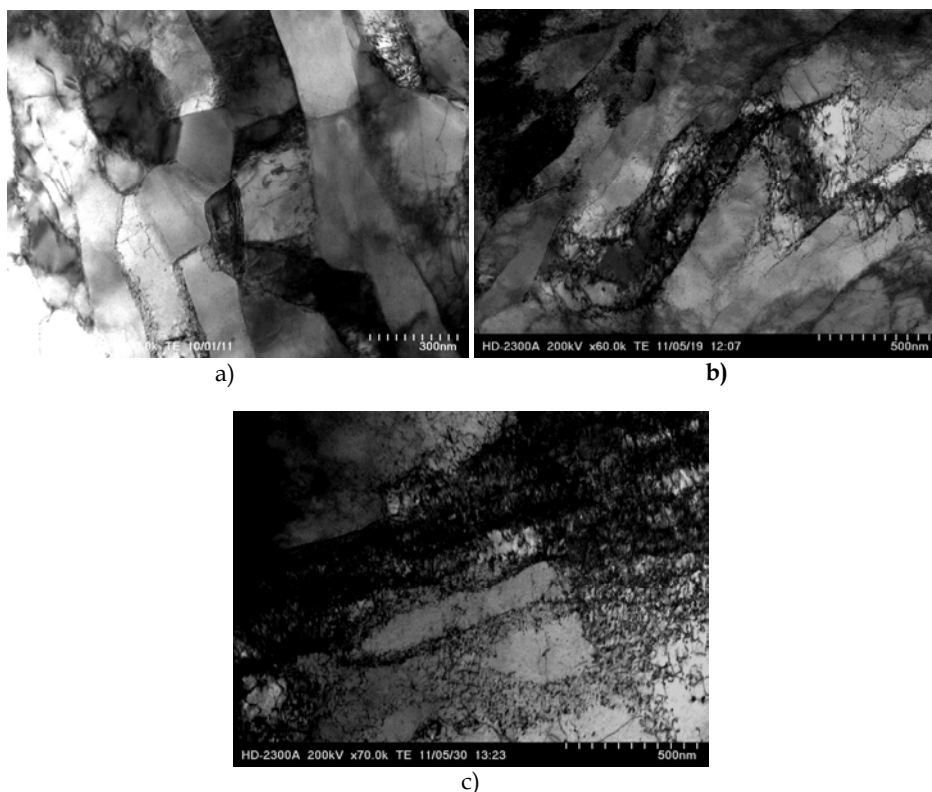


Fig. 21. Microstructure of Cu after COT deformation at: a) $v=0,04 \text{ mm/s}$, b) $0,1 \text{ mm/s}$, c) $0,6 \text{ mm/s}$ and constants: $f=1,6 \text{ Hz}$, $\alpha = 6^\circ$ and $\Delta h=7 \text{ mm}$

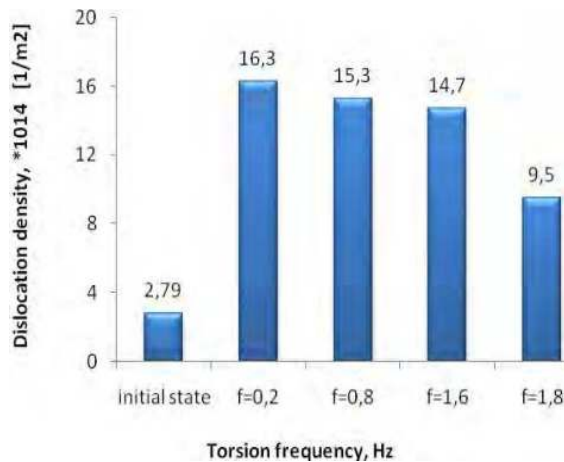


Fig. 22. The variation of the dislocation density In COTes samples with deferent value of torsion frequency and constant $\alpha = 6^\circ$, $v = 0,04$ mm/s and $\Delta h = 7$ mm

4.3 The absolute deformation

The absolute deformation is the parameter, the increase of which has an impact on the increase of the value of ε_f parameter. According with literature, the heterogeneity is connected with too small effective deformation [Kuziak, 2005]. Using larger effective deformation leads to the homogenization of the microstructure and larger grain refining. Analyzing the selected samples of the size distribution of the subgrains (Fig.23), grains (Fig.24), and the shape indicator (Fig.25) using the EBSD technique, it is seen that the microstructure after applying a larger absolute deformation, is characterized by greater homogeneity. The homogenous character of the microstructure is indicated by the narrow spectrum of the size distribution in subgrains/grains and shape indicator. In the samples which are deformed to lower values of the absolute deformation, the great diversity of grain and subgrain size is observed.

The effect connected with the accumulation of the deformation through the increase of Δh is, above all, the grains fragmentation by the generation of the dislocation boundaries. The structures obtained after the absolute strain $\Delta h = 3$ mm, are characterized by the initial stage of creating the DDWs boundaries (Fig.26). In the inside of the areas that are divided by the dislocation boundaries, the cellular dislocation structure can be seen (Fig.26). After applying the deformation $\Delta h = 7$ mm, the dislocation boundaries indicate a clear contrast proving the accumulating within the dislocation boundaries. A frequent intersection of the dislocation boundaries is observed (Fig.27).

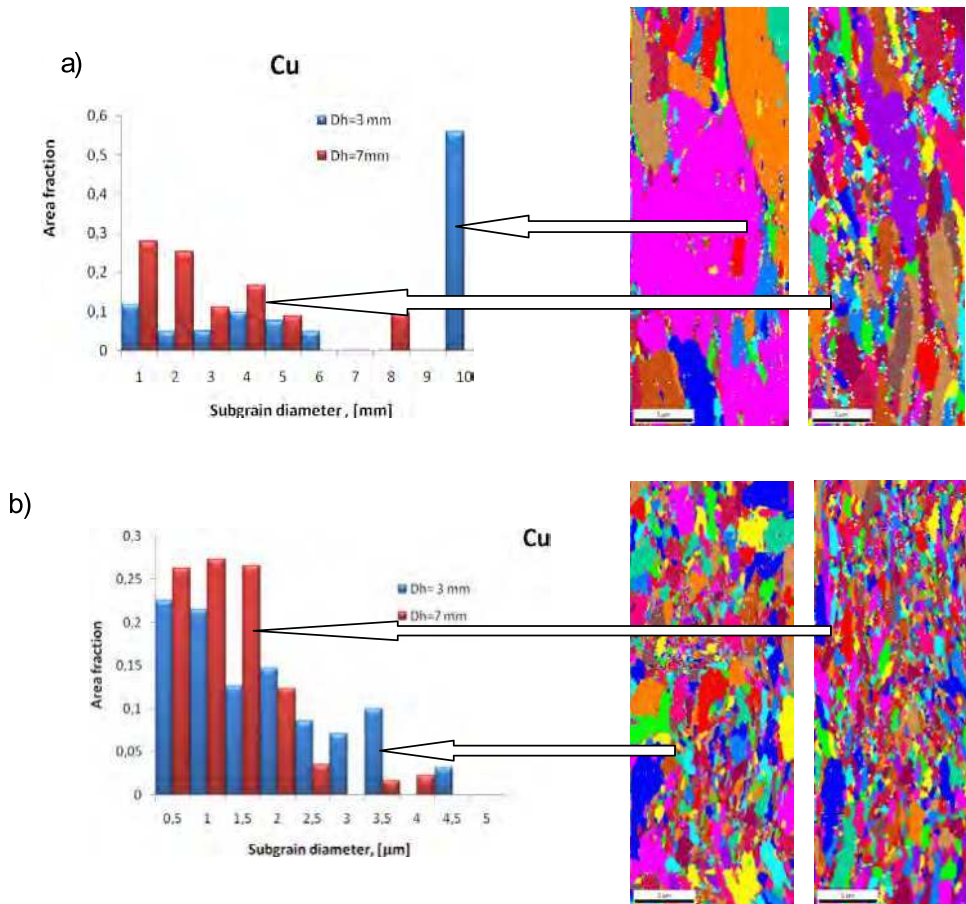


Fig. 23. Area fraction subgrains distributions of COTed Cu samples at: $\Delta h= 3\text{mm}$, $\Delta h= 7\text{mm}$; and at constant parameters: a) $f=0,8\text{ Hz}$, $\alpha =6^\circ$, $v=0,04\text{ mm/s}$, b) $f=1,6\text{ Hz}$, $\alpha =6^\circ$, $v=0,04\text{ mm/s}$

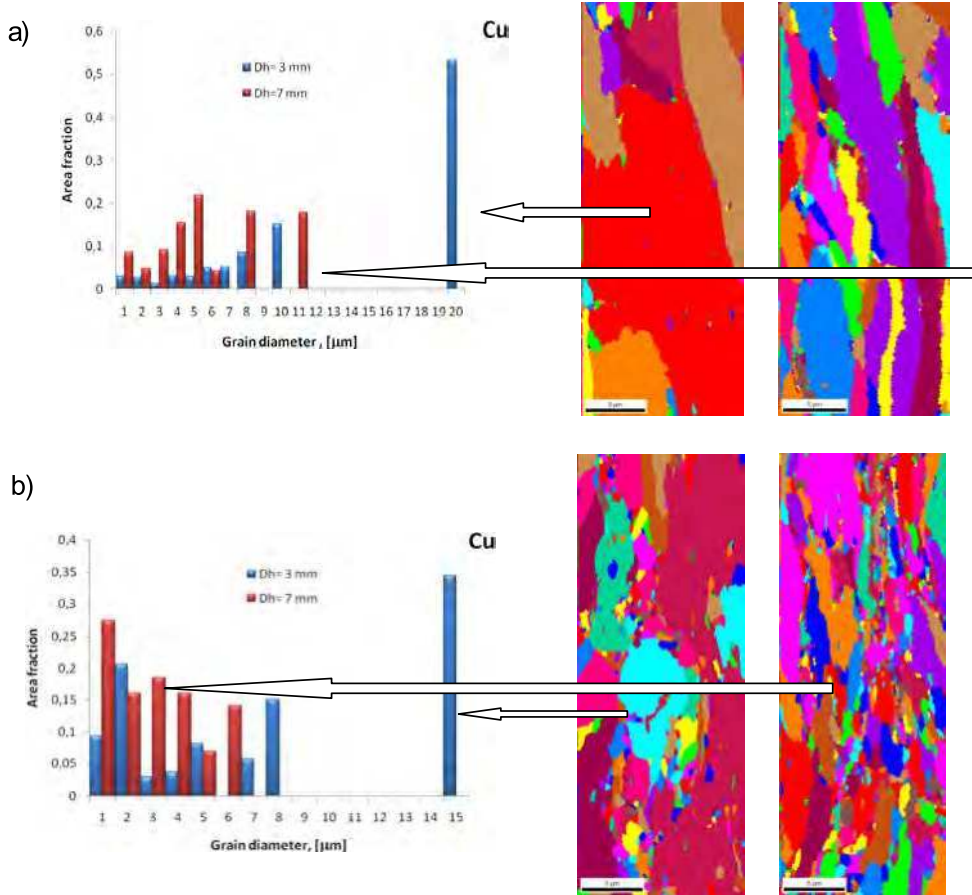


Fig. 24. Area fraction subgrains distributions of COTed Cu samples at: $\Delta h=3\text{ mm}$, $\Delta h=7\text{ mm}$; and at constant parameters: a) $f=0,8\text{ Hz}$, $\alpha=6^\circ$, $v=0,04\text{ mm/s}$, b) $f=1,6\text{ Hz}$, $\alpha=6^\circ$, $v=0,04\text{ mm/s}$

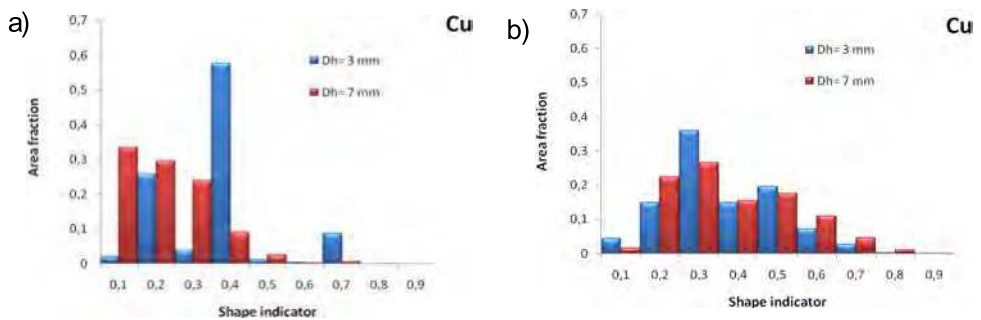


Fig. 25. Shape indicator distributions of COTed Cu samples at: $\Delta h=3\text{ mm}$, $\Delta h=7\text{ mm}$; and at constant parameters: a) $f=0,8\text{ Hz}$, $\alpha=6^\circ$, $v=0,04\text{ mm/s}$, b) $f=1,6\text{ Hz}$, $\alpha=6^\circ$, $v=0,04\text{ mm/s}$

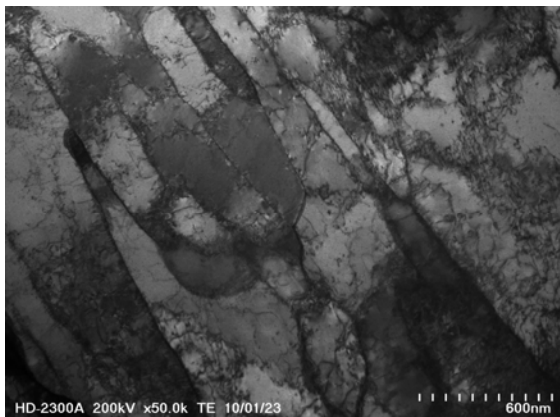


Fig. 26. Microstructure of Cu after COT deformation at: $f=1,6$ Hz, $\alpha =6^\circ$, $v=0,04$ mm/s and $\Delta h=7$ mm

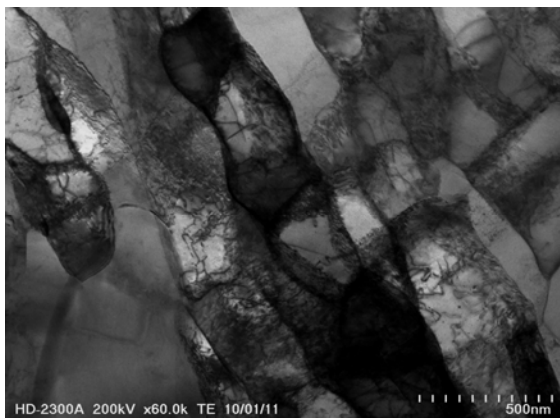


Fig. 27. Microstructure of Cu after COT deformation at: $f=1,6$ Hz, $\alpha =6^\circ$, $v=0,04$ mm/s and $\Delta h=7$ mm

The above data shows that for the effective structure refining, it would be beneficial to lead the deformations with:

- the torsional frequency 0,8 Hz and 1,6 Hz. The large equivalent deformations realized by the increase of the torsional frequency ranging from 0,8 Hz to 1,6 Hz, have an impact on the increase of the misorientation value between the created grains (Fig.20), on the increase of the area fraction of the grains with the average diameter up to $1\mu\text{m}$ (Fig.19), on the creation of the equiaxed grains and subgrains in a range of the ultrametric sizes (Fig.18).
- the high value of the absolute deformation ($\Delta h=7$ mm). The increase of the effective deformation by means of the increase of the absolute strain has an influence on the raise of the high-angle boundaries fraction, the increase of the defects, and the generation of the dislocation boundaries which are subject to the mutual intersection (Fig.26,27). The microstructures are characterized by great homogeneity (Figs.23-25).

- the low compression velocity up to approximately 0,04 mm/s. The deformation when the compression velocities are higher than 0,04 mm/s has no positive influence on refining a grain to the ultrametric level (Fig.16b.c). However, the deformation proceeding when the compression velocities are very slow, fosters the structure recovery processes (Fig.6d).

Taking into account the most convenient conditions of the Cu grain refining process it should be stated that:

- the average diameter of the Cu grains and subgrains equals correspondingly about 300 nm and 200 nm.
- the area fraction of the grain which has the ultrafine-grained size, is 60%
- the fraction of high -angle boundaries (HAB) reaches up to about 50%

Despite the majority of the literature data does not discuss the created grain/subgrain separately but rather give the overall values, it should be stated that the obtained are comparable with the literature data [Dobatkin, 2007; Dalla Torre, 2004].

Less attention is paid to determine the fraction of high angle boundaries (HAB) while describing the structural effects. Only the work of Richert [Richert, 2006] and Dobatkin [Dobatkin, 2007] proved that the fraction of high angle boundaries (HABs) in Cu is above 50%. It is difficult to relate the obtained data concerning the area fraction of the ultrametric grains to the literature data because the available literature does not give such results.

The demonstrated decrease of a dislocation density with the increasing deformation, argues for the recovery processes accompanying deformation. The literature also tells about the decrease of the dislocation density after obtaining large deformations [Dalla Torre, 2004].

5. Copper mechanical properties after compression with oscillatory torsion

The measurements of hardness for Cu which was subjected to compression with oscillatory torsion, shows that the changes of hardness depends both on the compression velocity and torsional frequency (Fig.28). The growth of the torsional frequency causes the gradual decrease of hardness. However, the increase of the compression velocity causes the increase of hardness. When the torsional frequency was $f= 0,2$ Hz, the levels of hardness were the highest - even 130 HV0,2. The material deformed when the values of f parameter are low, does not create the grain/subgrain structure but is only characterized by numerous dislocation tangles. Thus, a large dislocation density is responsible for high hardness. The growth of the effective deformations ε_f caused by the increase of the torsional frequency does not contribute to the increase of hardness. A slow decrease of hardness that was observed is connected with the reduction of the dislocation density resulting from the recovering processes that it undergo. The data shown in the Fig.29,30 suggests that the refined grain of Cu leads to 1,5 fold increase of the ultimate tensile strength (UTS) when compared with the initial stage. It was also stated that the highest increase of the mechanical properties accompanies the deformed material when the compression velocities are higher. In general, the increase of deformation realized through the increase of the torsional frequency does not increase the UTS and yield stress (YS) of the tested materials.

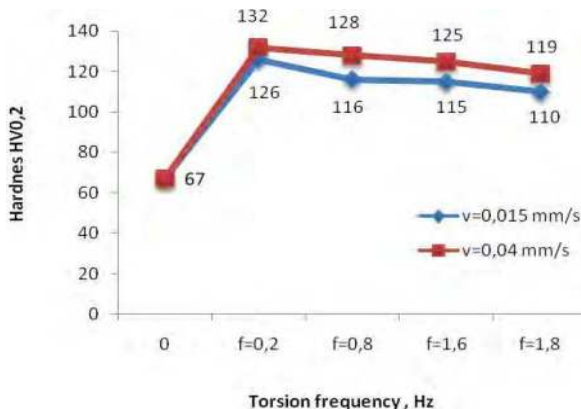


Fig. 28. Hardnes plotted as a function of torsion frequency and compression velocity; constants rest parameters: $\alpha = 6^\circ$, $\Delta h = 7$ mm

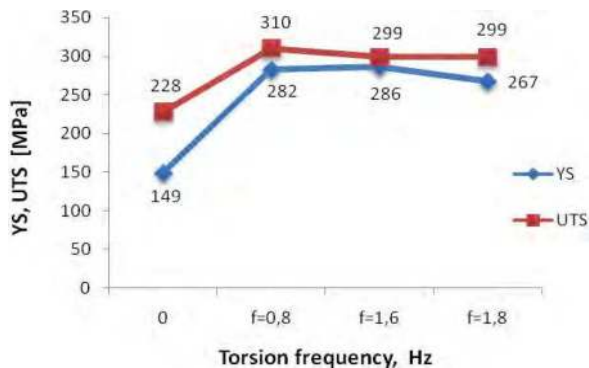


Fig. 29. YS and UTS plotted as a function of torsion frequency; constants rest parameters: $v = 0,015$ mm/s, $\alpha = 6^\circ$, $\Delta h = 7$ mm

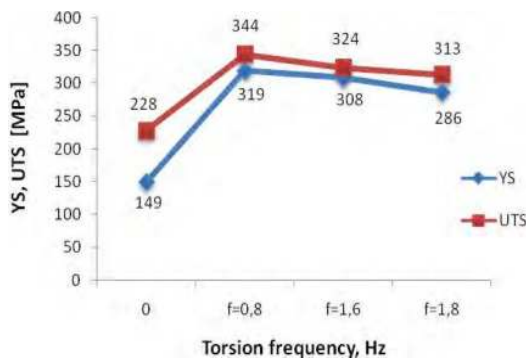


Fig. 30. YS and UTS plotted as a function of torsion frequency; constants rest parameters: $v = 0,04$ mm/s, $\alpha = 6^\circ$, $\Delta h = 7$ mm

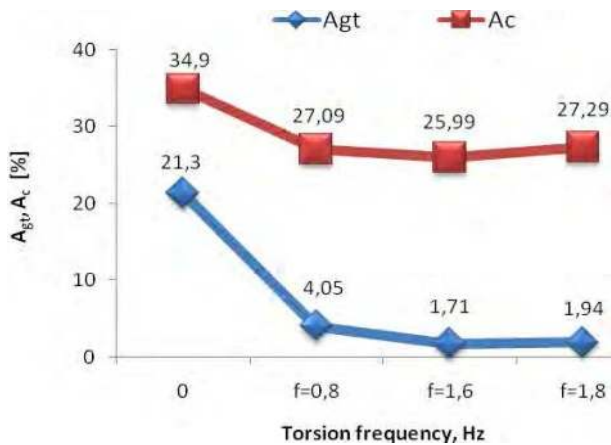


Fig. 31. A_{gt} , A_c plotted as a function of torsion frequency; constants rest parameters: $v=0,015$ mm/s, $\alpha=6^\circ$, $\Delta h=7$

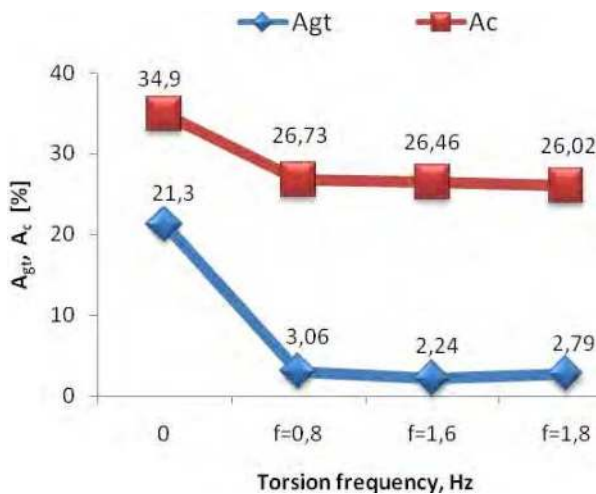


Fig. 32. A_{gt} , A_c plotted as a function of torsion frequency; constants rest parameters: $v=0,04$ mm/s, $\alpha=6^\circ$, $\Delta h=7$

The reason of low ductility of the material deformed by the SPD techniques is the localization of deformation. In the case of ultrafine-grained materials with the average diameter of the grain not exceeding 1000 nm, the elongations are usually bigger than in the case of nanograined materials. It is caused by the greater abilities of the material to cumulate the dislocations in grains what leads to higher velocity of the work hardening. The Cu plasticity expressed by the elongation to the rupture A_c is lower in comparison to the initial state and does not change with the variable of deformation parameters (Fig. 31 and Fig. 32). However, the total uniform elongation A_{gt} reaches value of about 2% (Fig. 31 and Fig. 32).

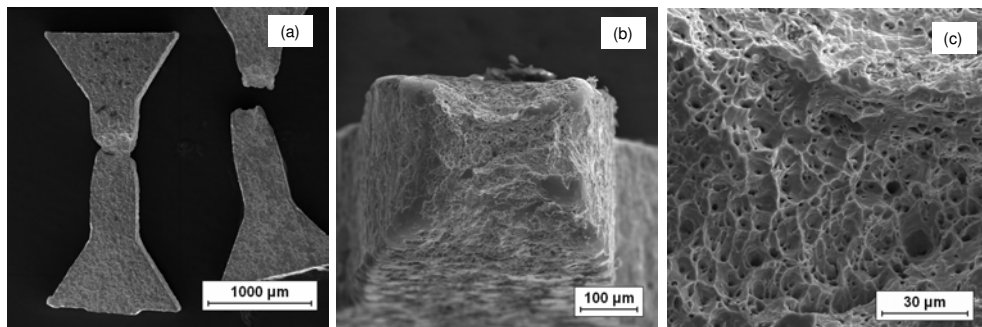


Fig. 33. Example fracture of the specimens 4 subjected to tension, b) necking near fracture section, c) fracture surface

Cracking of the materials after the tensile test happens in the areas of the measured parts (Fig. 33a). The material loses its stability as a result of the deformation localization in form of a neck which concentrates almost whole plastic deformation. In connection with that, the uniform elongation is negligible, however, the (Y_S) is close to the (UTS) . The fracture surface prove the ductile character (Fig. 33b,c).

The mechanical properties of Cu after the deformation ensures the best grain size reduction is when $f=1,6$ Hz, $\Delta h=7$, $\alpha=6^\circ$, $v=0,04$ reaches values of about: $Y_S=308$ MPa and $UTS=324$ MPa. The average UTS of Cu after the ECAP deformation is about 400 MPa [Kurzydłowski, 2004], and sometimes even higher values were noted [Berestercei, 2008]. The plastic properties, especially the uniform elongation for Cu, reaches the values of about 2%. This is the value comparable with the literature data [Kurzydłowski, 2004].

6. The mechanism of producing ultrafine-grained structures after the COT deformation

A lot of place in the structural tests is devoted to the mechanisms of grain-refining with the help of large SPD deformations. This matter is interesting particularly because of the application of different materials and different SPD techniques. The most important conclusions taken from the researches on the mechanisms of grain-refining are as follows:

- The fragmentation of grain takes place when the dislocation boundaries taking different forms are generated.
- The deformation is accompanied by the processes of dynamic recovery or even recrystallization [Kaibyshev, 2005, Wang, 2003]. An example of a material in which the grain-refining is the effect of deformation and of the „extended recovery” is aluminum. Whereas, in copper recrystallized grains are visible in the background of the deformed structure.
- The increase of misorientation happening thanks to the rotation of the grains boundaries and is a diffusion- controlled process. It is based on annihilation and absorption of the dislocation through the grains boundaries.

Hughnes and Hansen [Hughnes, 2000] presented the concept of microstructure evolution for the classic techniques of deformation which is based on the generation of dislocation boundaries which lead to the division of the initial grains into smaller volumes.

The proposed conception of the structure evolution is also characteristic for SPD techniques because many researchers dealing with refining the grain using large plastic deformations, introduce to the description of the structure the terminology in a form of the shear bands or dislocation layers. In general, there are three main mechanisms of the material structure-refining that are known:

- the production of new grains takes place thanks to a gradual increase in misorientation of dislocation boundaries as a result of absorption of new dislocations created during the deformation [Xu, 2005],
- the fragmentation of grains takes place thanks to the generation of the shear bands [Richert, 2006],
- the fragmentation of grains takes place thanks to the production of new grains as a result of the continuous recovery or continuous recrystallization [Kaibyshev, 2005, Wang, 2003].

The refining of the copper grain after the COT deformation, happens as a result of the generation of dislocation boundaries, which together with the growth of deformation transform themselves into ultrafine-grained structure. The introductory stage of the grain-refining is the creation of DDWs dislocation walls the misorientation of which reaches even a few degrees and they stretch along the considerable fraction of a grain, separating blocks of dislocation cells (CBs) (Fig.34). Within the boundaries a high density of dislocation is accumulated (Fig.34).

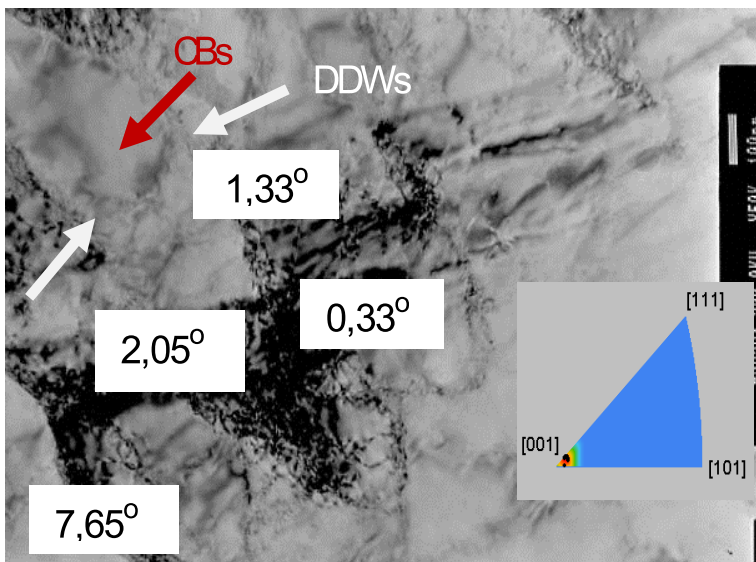


Fig. 34. Microstructure of Cu after COT deformation at: $f=0,2$ Hz, $v=0,015$ mm/s, $\alpha=6^\circ$, $\Delta h=7$ mm

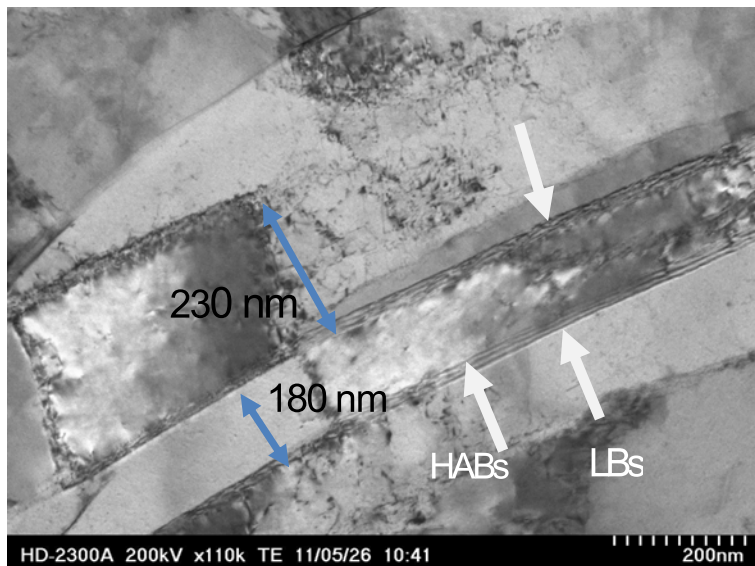


Fig. 35. Microstructure of Cu after COT deformation at: $f=0,8 \text{ Hz}$ $f=0,2 \text{ Hz}$, $v=0,015 \text{ mm/s}$, $\alpha=6^\circ$, $\Delta h=7 \text{ mm}$

The growth of deformation causes the transformation of the DDWs dislocation walls into lamellar boundaries (LBs) which has larger misorientation (sometimes above 15° - HABs) which resembles long subgrains (Fig.35) Inside of the lamellar boundaries, the dislocation structure is regular and singular dislocation cells are usually noticeable. Moreover, the distance between the lamellar areas decreases (Fig.35). It can be assumed that the accumulation of deformation induces not only the creation of new dislocation boundaries and high angle boundaries but above all, it induces the crossing of dislocation boundaries. This phenomenon of intensive boundaries crossing (Fig.36) is a result of activating the subsequent slip systems while the process of deformation. The places where the dislocation boundaries are crossing induce the generation of almost equiaxed subgrains/grains (Fig.37). As a result, the large deformation increases the share of grains/subgrains boundaries and misorientation scattering (Fig.6) This, in turn, leads to the formation of the grains with HABs boundaries (Fig.37). The result of EBSD test shown in the Fig.6 and Fig.17 also constitute the confirmation of the tests. On the basis of EBSD tests it was proved that in a great deal of cases elongated neighboring grains remain in crystallographic compatibility. In the case of fine, equiaxed grains, the orientation was accidental (Fig.6).

The high-angle boundaries (HABs) marked in the Fig.36, 37 have bulges characteristic for the dynamic recrystallization and they can indicate the migration of high-angle boundaries. In many works it was proven that the migration of the grain boundaries created as a result of SPD process as an effect of dynamic recrystallization [Kaibyshev, 2005; Wang, 2003]. The sequence of figures registered during the rotation of the sample at a given angle indicates that the bulges of HAB boundaries are not the effects of the boundary migration but of the mutual superimposing of the boundaries which are in one crystallographic orientation in a given microarea (Fig.38).

This means that the creation of ultrafine-grained structures using the COT method is not determined by the process of recrystallization.

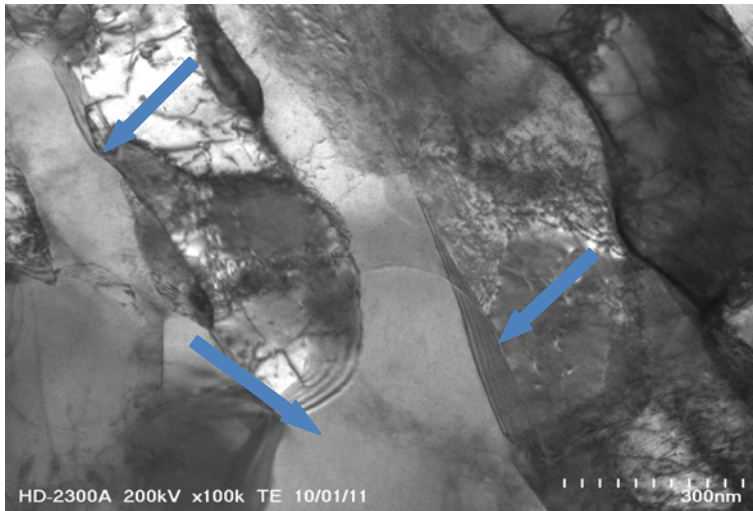


Fig. 36. Microstructure of Cu after COT deformation at: $f=0,8\text{Hz}$, $v=0,015\text{ mm/s}$, $\alpha=6^\circ$, $\Delta h=7\text{ mm}$

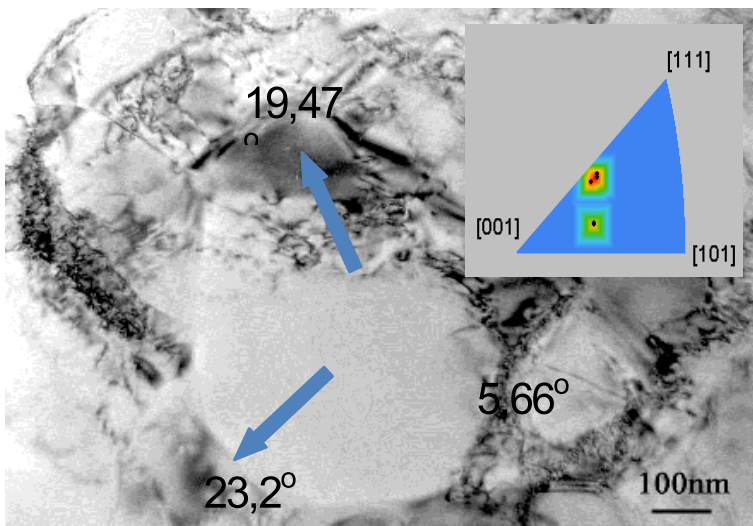


Fig. 37. Microstructure of Cu after COT deformation at: $1,6\text{ Hz}$, $v=0,015\text{ mm/s}$, $\alpha=6^\circ$, $\Delta h=7\text{ mm}$

In order to trace the way in which the low-angle boundaries (LABs) change into HABs boundaries, a series of structural tests was carried out in which the Kikuch diffraction was used. Some examples are presented in the Fig. 39. Defining of the local orientations and crystallographic misorientations of particular areas, allowed to formulate the mechanism in which the high-angle boundaries are formed. The examples presented in Fig.39 suggest that the recovery of Cu caused by EBU happens relatively slow. That is why the dislocations generated during the deformation do not easily annihilation. The cellular type of the dislocation structure remains even if a large deformation is used. The EBSD tests show that the fraction of LABs boundaries is still present even after a large deformation (Fig.9,20).

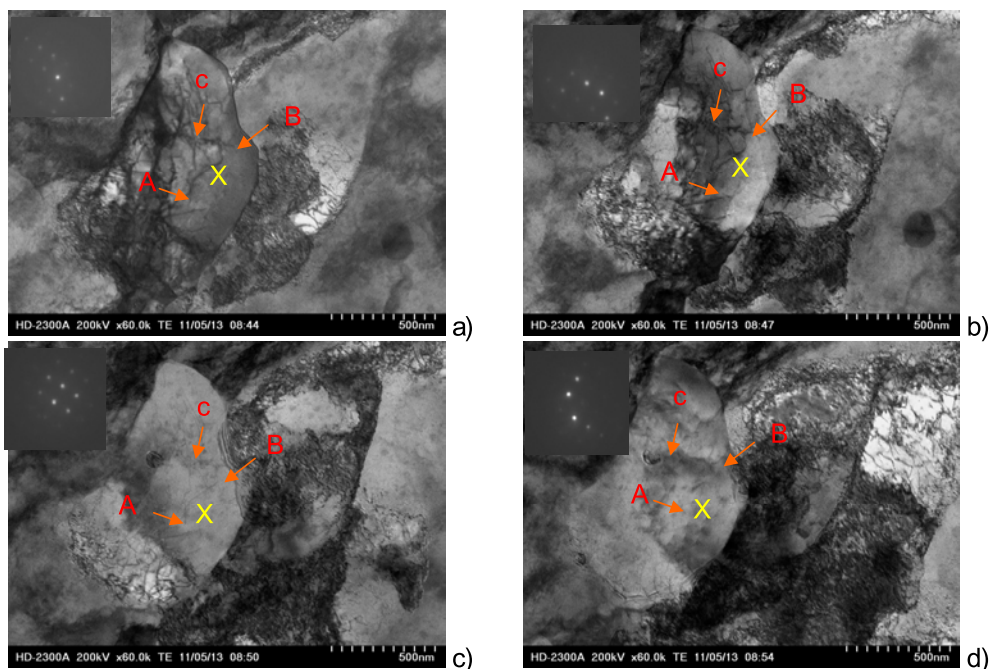


Fig. 38. Microstructure of Cu after COT deformation at: 0,8 Hz, $v=0,15$, $\alpha=6^\circ$, $\Delta h=7$ mm. ABC marked grains are visible after changes in sample rotation : a) $\alpha= -3,9^\circ$, b) $\alpha= -6,2^\circ$, c) $\alpha= -9,6^\circ$, d) $\alpha= -10,2^\circ$. Diffraction patterns taken from X

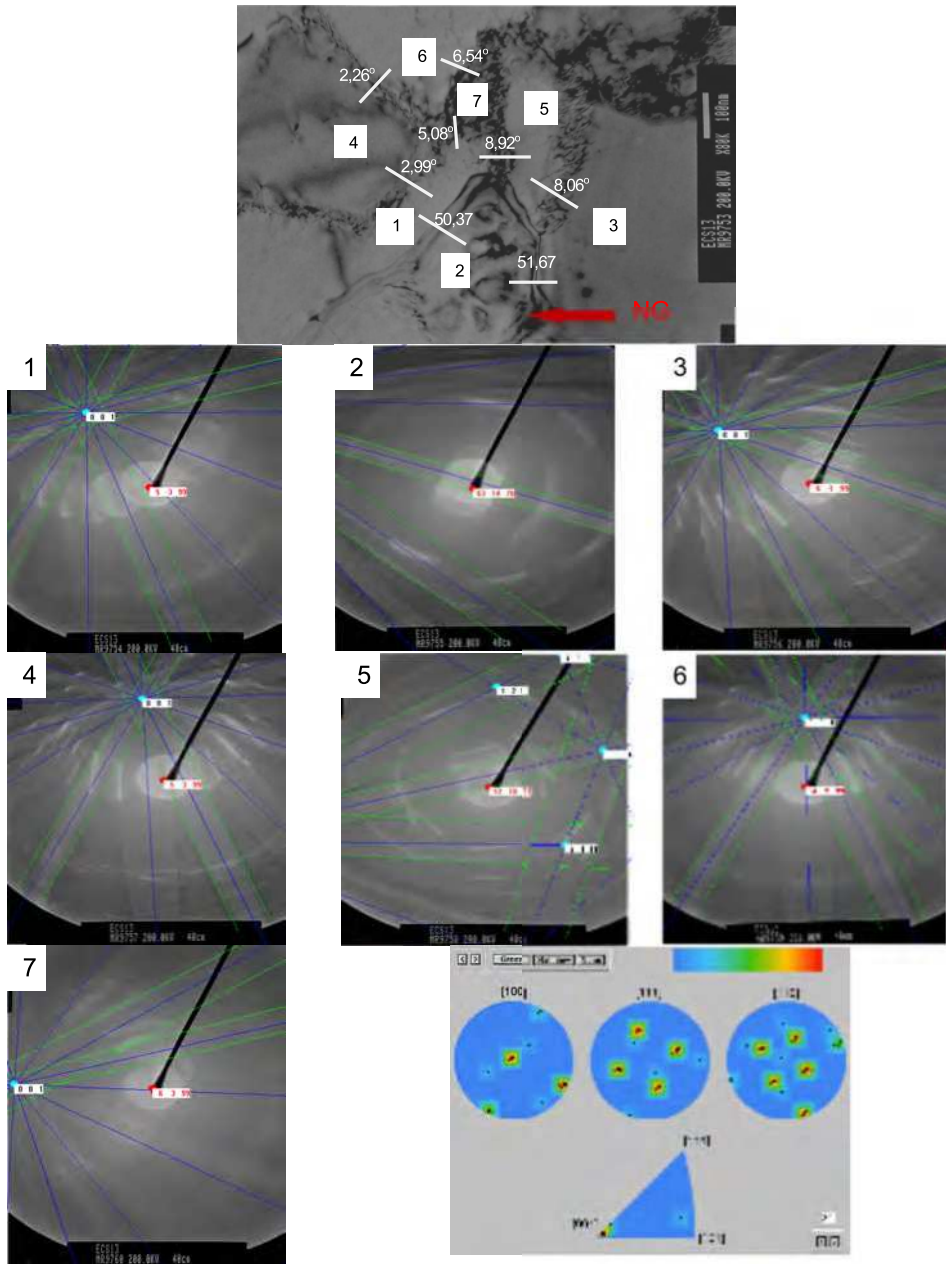


Fig. 39. a) Microstructure of Cu after COT deformation at: $f = 1,6$ Hz, $\alpha = 6^\circ$, $v = 0,04$ mm/s. High misorientation of nonequilibrium grain boundary in grain marked 2.; b) Kikuchi diffractions with solutions. Numbers 1-7 in Fig. 38a corresponds Kikuchi patterns 1-7 ; c) orientation of analyzed area

The clusters of dislocation are usually created near the boundaries what causes nonequilibrium state of the grains boundaries. A weak and heterogeneous diffractonal contrast inside of the grains indicates a high level of the interior stress in the grain boundaries (Fig.39). Such boundaries are high-angular but almost invisible.

The structural analysis presented here show that the dominating mechanism of forming the high-angle grains in Cu is the growth of misorientation in dislocation boundaries. This, in turn, happens as an effect of absorbing dislocations to the grains boundaries during the deformation process. The nonequilibrium boundaries presented in the Fig.39 are formed from the absorption of numerous dislocations as a result of glide and climb [32].

It was proven that together with the growth of deformation, the fraction of the boundaries increases gradually from 5° - 15° (up to approx. 30%) and the fraction of HABs boundaries raises above 15° (to about 40%) (Fig.6). Approximately, on a constant level the fraction of narrow-angle boundaries LABs is formed and it does not exceed 30%. When the process parameters are changed (Fig.20) the increase of the HABs fraction to 50% is visible, but also the fraction of boundaries form 5° - 15° was reduced to approximately 20%.

The LABs boundaries still constituted 30%. It can mean that the boundaries with misorientation from 5° - 15° transform themselves into the grain boundaries. Because of the fact that the boundaries with an average misorientation (5° - 15°) are the nonstable boundaries [Cao, 2008], as a result of the deformation they are transformed into high-angle boundaries.

7. Summary

The chapter concentrates on the possibility of a structure forming and on the properties of the metallic materials by means of using the method of compression with oscillatory torsion. The issues that were introduced have a great technical importance because it refers to the formation of ultrafine-grained structure by application of the unfamiliar SPD technique. Because the intensive research on generating new, more economical methods of producing ultrafine-grained materials, the presented matter coincides with the current state of research conducted in many scientific centers.

The aim of the tests in which the COT deformation method was used, was to obtain maximal refining of the grain below $1\mu\text{m}$. The structural investigations showed that using the COT method, the grains of the Cu can be refined to ultrafine-grained. The intensity of grain-refining depends on the value of the effective deformation, however, the deformation path (the selection of the deformation parameters) is a decisive factor.

Using the different deformation parameters in process the presence of different phenomena that were controlling the growth of the microstructure. The increase of deformation (realized through the Hz growth) causes a progress in the grain refinement. The deformation conducted when the torsional frequencies were 0,8 Hz and 1,6 Hz is the most beneficial for obtaining the most refined grain. Using a significantly higher torsional

frequency -18 Hz during the deformation caused considerable restrictions in the grain-refining because of the intensive recovery which begins to dominate over the deformation process.

It can be noticed that a relatively small change of the compression velocity, had an impact on considerably greater refining of the structure. The acceleration of the deformation process by increasing the compression velocity, causes the delay of the structure recovery process. What is seen through the changes of dislocation density for example. Despite reducing the effective deformation, the progress in the structure refining is observed what denies the results described in the literature [Dalla Tore, 2004; Wang, 2003]. However, the next increase of the compression velocity from 0,1 mm/s and 0,6 mm/s does not foster grain-refining. It should be explained by the fact that the effective deformation is too small.

The main effect of deformation is the increase of the structure's homogeneity. The homogeneity is obtained mainly by the increase of the height parameter Δh .

When the process parameters are as follows: the torsional frequency ranges from 0,8 Hz to 1,6 Hz; $\Delta h=7\text{mm}$, and the compression velocity ranges from 0,015 to 0,04 mm/s; the maximal refining of the copper grain is obtained but also:

- the average diameter of the grain/subgrain correspondingly 200 nm and 300 nm.
- the share of high-angle boundaries is about 50% and
- the fraction of the ultrafine grains is about 60%. In spite of using large equivalent deformations, narrow-angle boundaries up to 15° constitute a significant fraction in both materials. The fraction of high-angle boundaries does not exceed 70%. This means that the thermal stability of the structures formed in such a way is sufficient [Raab, 2004; Lugo, 2008].

The result of mechanical tests were discussed in details for selected schemes of deformation in which the effects of deformation were visible the most. The influence of grain refining on the mechanical properties of the grain, was determined on the basis of the hardness measurements and the tensile test of the micro samples. The results of the mechanical tests that were carried out, indicate clearly that the changes taking place in the structure and the grain refining had a positive influence on the mechanical properties of the tested materials. However, the uniform elongation is not strongly dependent on the grain refining.

The difference in the properties that were observed, mainly result from using different schemes of deformation.

The results of structural investigations were the basis for determining the mechanisms of grain refining and forming high-angle boundaries. It was proven that the formation of ultrafine grains during the COT deformation is based on the general mechanisms of forming the dislocation boundaries. The process of grain refining proceeds by the generation of the LABs and HABs boundaries. In the introductory stage of deformation the dislocation boundaries are formed which are perpendicular to the direction of the compression force. The formation of the dislocation boundaries which proceed in such a way, suggests that in the initial stage of deformation it is mainly the compression that initiates the process of the grain refining. The non-directional process of deformation

(the introduction of an additional torsion causing the change in the direction of loading) leads to the deformation of the material in more and more numerous systems of glides and to the new dislocations having influence on the active system of glides on the previously-generated dislocations. The effect of the introduced, additional loading is the increase in the number of the dislocation boundaries that cross mutually. When the effective deformation in the microstructure increases, the distances between the dislocation boundaries decrease – a new order of LBs dislocation boundaries is created which as a result of the thermal process activation (recovery), transform themselves into subgrains and grains. The process leads to the increase of misorientation of the grain's boundaries.

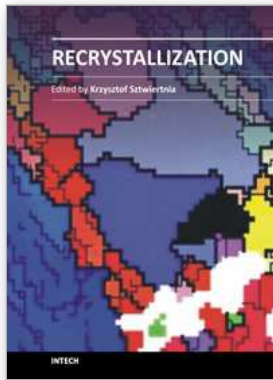
A significant role in forming the ultrafine-grained structure has the recovery process. Dislocations are rearranged, undergo annihilation and are also absorbed to the grain boundaries. Such a rebuilding of a dislocation structure causes the increase of the misorientation within the grain boundaries.

8. References

- Pakiela, Z. (2009). *Mikrostrukturalne uwarunkowania właściwości mechanicznych nanokrystalicznych metali*, Oficyna Wydawnicza Politechniki Warszawskiej
- Olejnik, L. et al. (2005). *Bulletin the polish academy of science, Technical sciences*, 53, pp. 413-423
- Bochniak, W. et al. (2005). *Journal of Materials Processing Technology*, 169, pp. 44-53
- Shaarbağ, M. et al. (2008). *Materials Science Engineering*, A473, pp. 28-33
- Raab, G.J. et al. (2004). *Mater. Sci. Eng.*, A 382, pp. 30
- Lugo, A. N. et al. (2008). *Materials Science Engineering*, A477, pp. 366-371
- Kulczyk, M. et al. (2007). *Materials Science Poland*, 25, pp. 991-999
- Pawlicki J. & F. Grosman. (2005). Naprężenia uplastyczniające metali w warunkach złożonych obciążeń, *Materiały XII Konferencji Informatyka w Technologii Metali*, Ustroń 16-19.01
- Grosman F. & Pawlicki J. (2004). Processes with forced deformation path. New Forming Technology 2004. *Proceedings of the 1st ICNFT, Harbin Institute of Technology Press*, Harbin, China, Sep. 6–9
- Rodak, K. & Goryczka T. (2007). *Solid State Phenom*, 130, pp. 111-113
- Ungar, T. et al. (2001). *Materials Science Engineering*, A319-321, pp. 274-278
- Kuziak, R. (2005). *Modelowanie zmian struktury i przemian fazowych zachodzących w procesach obróbki cieplno-plastycznej stali*, Instytut Metalurgii Żelaza, Gliwice
- Dobatkin, S. V. et al. (2007). *Materials Science Engineering*, A462, pp. 132-138
- Dalla Torre, F. (2004), *Acta Materialia*, 52, pp. 4819- 4832
- Richert, M. (2006). *Inżynieria nanomateriałów i struktur ultra drobnoziarnistych*, Uczelniane Wydawnictwo Naukowo Techniczne, Kraków
- Kurzydłowski, K. J. (2004). *Biuletin of the polish academy of sciences technical sciences*, 52, pp. 301-311
- Beresterci, M. et al. (2008). *Metalurgija*, 47, pp. 295-299
- Kaibyshev, R. et al. (2005). *Materials Science Engineering*, A398, pp. 341-351
- Wang, G. et al. (2003). *Materials Science Engineering*, A346, pp. 83-90
- Hughnes, D.A. et al. (2000). *Acta Materialia*, 48, pp. 2985-3004

Xu, Ch. et al. (2005). *Materials Science Engineering*, A398, pp. 66-76

Cao, W.Q. et al. (2008). *Materials Science Engineering*, A492, pp. 74-79



Recrystallization

Edited by Prof. Krzysztof Sztwiertnia

ISBN 978-953-51-0122-2

Hard cover, 464 pages

Publisher InTech

Published online 07, March, 2012

Published in print edition March, 2012

Recrystallization shows selected results obtained during the last few years by scientists who work on recrystallization-related issues. These scientists offer their knowledge from the perspective of a range of scientific disciplines, such as geology and metallurgy. The authors emphasize that the progress in this particular field of science is possible today thanks to the coordinated action of many research groups that work in materials science, chemistry, physics, geology, and other sciences. Thus, it is possible to perform a comprehensive analysis of the scientific problem. The analysis starts from the selection of appropriate techniques and methods of characterization. It is then combined with the development of new tools in diagnostics, and it ends with modeling of phenomena.

How to reference

In order to correctly reference this scholarly work, feel free to copy and paste the following:

Kinga Rodak (2012). The Effect of Strain Path on the Microstructure and Mechanical Properties in Cu Processed by COT Method, *Recrystallization*, Prof. Krzysztof Sztwiertnia (Ed.), ISBN: 978-953-51-0122-2, InTech, Available from: <http://www.intechopen.com/books/recrystallization/the-effect-of-strain-path-on-the-microstructure-and-mechanical-properties-in-cu-processed-by-cot-met>

INTECH
open science | open minds

InTech Europe

University Campus STeP Ri
Slavka Krautzeka 83/A
51000 Rijeka, Croatia
Phone: +385 (51) 770 447
Fax: +385 (51) 686 166
www.intechopen.com

InTech China

Unit 405, Office Block, Hotel Equatorial Shanghai
No.65, Yan An Road (West), Shanghai, 200040, China
中国上海市延安西路65号上海国际贵都大饭店办公楼405单元
Phone: +86-21-62489820
Fax: +86-21-62489821

© 2012 The Author(s). Licensee IntechOpen. This is an open access article distributed under the terms of the [Creative Commons Attribution 3.0 License](#), which permits unrestricted use, distribution, and reproduction in any medium, provided the original work is properly cited.